

The Alignments of the Galaxy Spins with the Real-Space Tidal Field Reconstructed from the Two Mass Redshift Survey

Jounghun Lee

Department of Physics and Astronomy, FPRD, Seoul National University, Seoul 151-747, Korea

jounghun@astro.snu.ac.kr

Pirin Erdogdu

School of Physics and Astronomy, University of Nottingham, University Park, Nottingham, NG7 2RD, UK

Pirin.Erdogdu@nottingham.ac.kr

ABSTRACT

We report a direct observational evidence for the existence of the galaxy spin alignments with the real space tidal field. We calculate the real space tidal field from the real space density field reconstructed recently from the Two Mass Redshift Survey (2MRS) by Erdogdu et al. in 2006. Using a total of 12122 nearby spiral galaxies from the Tully Galaxy Catalog, we calculate the orientations of their spin axes relative to the 2MRS tidal field. We find a clear signal of the intrinsic correlations between the galaxy spins and the intermediate principal axes of the tidal shears. The null hypothesis of no correlation is rejected at 99.99% confidence level. We also investigate the dependence of the intrinsic correlations on the galaxy morphological type and the environment. It is found that (i) the intrinsic correlation depends weakly on the morphological type of the spiral galaxies but tends to decrease slightly as the type increases; (ii) it is stronger in the high-density regions than in the low-density regions. The observational result is quantitatively consistent with analytic prediction based on the tidal torque theory. It is concluded that the galaxy spin orientations may provide in principle a new complimentary probe of the dark matter distribution.

Subject headings: galaxies:structure — large-scale structure of universe

1. INTRODUCTION

The seeds of the galaxies observed in the present universe are the tiny- amplitude inhomogeneities of the primordial density field which are presumably generated by the quantum fluctuations during the inflation (Guth & Pi 1982). The amplitudes of the density inhomogeneities grew gradually via gravity after recombination to form proto-galaxies in the initially overdense regions. Provided that the shapes of the proto-galaxies were not perfectly spherical, the tidal torques from the surrounding matter generated the spin angular momentum from the proto-galaxies at first order (Peebles 1969; Doroshkevich 1970; White 1984). In consequence, the proto-galaxy spin axes came to be correlated with the principal axes of the local tidal shear tensors defined as the second derivative of the gravitational potential field (Dubinski 1992; Lee & Pen 2000).

The tidal effect from the surrounding matter continued till the turn-around moment when the proto-galaxies got separated from the neighborhood and began to collapse. If the spin angular momentum were well conserved after the turn-around moment, the spin directions of the galaxies at present epoch would still possess the initially induced correlations with the local tidal shears. In the subsequent evolution, however, it is likely that the complicated nonlinear processes may have modified significantly the directions of the spin angular momentum, decreasing the degree of the spin-shear alignments (Porciani et al. 2002). A critical issue to address is whether the initially induced spin-shear alignments still remain to a non-negligible degree or not.

Several attempts so far have been made to measure the intrinsic alignments of the galaxy spins numerically (Lee & Pen 2000; Porciani et al. 2002; Patiri et al. 2006; Aragon-Calvo et al. 2007; Brunino et al. 2007; Hahn et al. 2007). For instance, using the simulated galactic halos in recent high-resolution N-body experiments, Porciani et al. (2002) investigated the correlations between their spin axes and the local tidal tensors and found that the spins of the simulated galactic halos at present epoch completely lost their memory of the intrinsic alignments with the initial tidal tensors.

In contrast, observational analyses have provided indirect evidences for the existence of the intrinsic alignments of galaxy spins at present epoch (Flin & Godlowski 1986, 1990; Navarro et. al. 2004; Aryal & Saurer 2005a,b; Trujillo et. al. 2006). It was Flin & Godlowski (1986, 1990) who first noted the anisotropic orientations of the spin axes with respect to the Local Supercluster plane. They found that the planes of the spiral galaxies tend to be perpendicular to the Local Supercluster plane. Recently, Navarro et. al. (2004) confirmed this effect, showing that the spin axes of the nearby edge-on spirals are inclined relative to the supergalactic plane (cf. Aryal & Saurer 2005a). Trujillo et. al. (2006) also recently reported an observational finding that the spin axes of the void galaxies tend to lie on the

void surfaces. These observational evidences are consistent with the tidal-torque picture that the large-scale structures have deep influences on the orientations of the nearby galaxy spin axes.

Yet, these previous approaches were only indirect and still inconclusive about the existence of the spin-shear alignments. First of all, in previous approaches, the orientations of the surrounding large scale structures were measured not in real space but in redshift space. The redshift-distortion effect could cause substantial uncertainty in the final results. Furthermore, these previous detections of the effect of the large-scale structure on the galaxy spins cannot be automatically translated into the detection of the initial tidal effect on the galaxy spins. To find a real signal of the spin-shear alignments, it is inevitable to measure directly the correlations between the galaxy spin axes and the local tidal shear tensors. In fact, it was Lee & Pen (2002) who attempted for the first time to measure directly the spin-shear alignments. But, their approach suffered from noisy reconstruction of the tidal field as well as inaccurate measurement of the spin axes of the spiral galaxies.

Very recently, the real space density field has been reconstructed from the densest galaxy redshift survey (Erdogdu et al. 2006), which may allow us to measure directly the intrinsic alignments of the galaxy spins with the tidal shear field with low statistical errors. Our goal here is to measure the intrinsic spin-shear correlations by reconstructing the real space tidal field from the 2MRS density field.

The plan of this Paper is as follows. In §2, we provide a concise overview of the linear tidal torque model. In §3, we present the observational results of the intrinsic spin-shear correlations from the 2MRS tidal field and the Tully Galaxy Catalog, and compare the observed signals with theoretical predictions. In §4, we summarize the achievements of our work and draw a final conclusion.

2. OVERVIEW OF THE ANALYTIC MODEL

In the linear tidal torque theory the spin angular momentum of a proto-galaxy is determined by its geometric shape and the tidal force from the surrounding matter distribution (Peebles 1969; Doroshkevich 1970; White 1984):

$$L_i = \epsilon_{ijk} T_{jl} I_{lk}, \quad (1)$$

where (L_i) is the spin angular momentum vector of a proto-galaxy, (I_{ij}) is the inertia momentum tensor representing the geometry of a proto-galactic region, and (T_{ij}) is the initial shear tensor representing the tidal torques from the surrounding matter.

In the principal axis frame of (T_{ij}) , equation (1) is written as

$$L_1 \propto (\lambda_2 - \lambda_3)I_{23}, \quad L_2 \propto (\lambda_3 - \lambda_1)I_{31}, \quad L_3 \propto (\lambda_1 - \lambda_2)I_{12}, \quad (2)$$

where $\lambda_1, \lambda_2, \lambda_3$ represent the three eigenvalues of (T_{ij}) with $\lambda_1 \geq \lambda_2 \geq \lambda_3$, and I_{12}, I_{23}, I_{31} are the off-diagonal components of (I_{ij}) expressed in the principal axis frame of (T_{ij}) . Since the absolute magnitude of $(\lambda_3 - \lambda_1)$ is the largest, equation (2) suggests that $|L_2|$ is the largest on average provided that the off-diagonal components, I_{12}, I_{23}, I_{31} , are not zero.

Hence, it is uniquely predicted by the linear tidal torque theory that the spin angular momentum of a proto-galaxy is intrinsically aligned with the intermediate principal axis of the local tidal shear tensor. As mentioned in §1, an important question to answer is whether this initially induced spin-shear alignments still remain at present epoch or not. In the frame of the linear tidal torque model, Lee & Pen (2000, 2001) have proposed the following generalized quadratic formula to quantify the expected degree of the intrinsic alignments between the spin axes of the galaxies and the intermediate principal axis of the local tidal tensor at present epoch:

$$\langle L_i L_j | \hat{\mathbf{T}} \rangle = \frac{1+c}{3} \delta_{ij} - c \hat{T}_{ik} \hat{T}_{kj}. \quad (3)$$

where $\mathbf{L} \equiv (L_i)$ is the galaxy spin angular momentum vector rescaled to be dimensionless, $\hat{\mathbf{T}} \equiv (\hat{T}_{ij})$ is the traceless tidal tensor rescaled to have unit magnitude, and $c \in [0, 1]$ is a correlation parameter to measure the strength of the intrinsic spin-shear alignments with the nonlinear modifications taken into account. For the unit spin $\hat{\mathbf{L}} \equiv (\hat{L}_i)$, the correlation parameter in equation (3) is reduced by a factor of 3/5 (Lee & Pen 2001). If c has its minimum value of zero, it corresponds to the case that the nonlinear effect completely broke the initial spin-shear correlations, so that the present galaxy spin axes have random orientations.

Using equation (3), Lee et al. (2005) have derived the following probability density distribution of the orientations of the galaxy spin vectors relative the tidal shear tensors:

$$p(\cos \alpha, \cos \beta, \cos \theta) = \frac{1}{2\pi} \prod_{i=1}^3 \left(1 + c - 3c\hat{\lambda}_i^2 \right)^{-\frac{1}{2}} \times \left(\frac{\cos^2 \alpha}{1 + c - 3c\hat{\lambda}_1^2} + \frac{\cos^2 \beta}{1 + c - 3c\hat{\lambda}_2^2} + \frac{\cos^2 \theta}{1 + c - 3c\hat{\lambda}_3^2} \right)^{-\frac{3}{2}}, \quad (4)$$

where $\hat{\lambda}_1, \hat{\lambda}_2, \hat{\lambda}_3$ are the eigenvalues of $\hat{\mathbf{T}}$, and α, β and θ represent the angles between $\hat{\mathbf{L}}$ and the major, intermediate, and minor principal axes of $\hat{\mathbf{T}}$, respectively.

To quantify the preferential alignment of $\hat{\mathbf{L}}$ with the *intermediate* principal axis of $\hat{\mathbf{T}}$, we calculate $p(\cos \beta)$: In equation (4) $\hat{\lambda}_i$'s ($i = 1, 2, 3$) satisfy the traceless condition of $\sum_i \hat{\lambda}_i = 0$

as well as unit-magnitude condition of $\sum_i \hat{\lambda}_i^2 = 1$. Therefore, they are well approximated as $\hat{\lambda}_1 = -\hat{\lambda}_3 = -1/\sqrt{2}$ and $\hat{\lambda}_2 = 0$. Putting these approximate values into equation (4), we derive the probability density distribution of $\cos \beta$ as

$$p(\cos \beta) = (1 + c) \sqrt{1 - \frac{c}{2}} \left[1 + c \left(1 - \frac{3}{2} \cos^2 \beta \right) \right]^{-3/2}, \quad (5)$$

where $\cos \beta$ is assumed to be in the range of $[0, 1]$ since what is relevant to us is not the sign of the spin vector but the relative orientation. If $c = 0$ the probability density distribution $p(\cos \beta)$ will be a uniform distribution of $p(\cos \beta) = 1$; If $c > 0$, then $p(\cos \beta)$ will increase toward $\cos \beta = 1$, indicating the existence of the preferential alignments of the galaxy spin axes with the intermediate principal axes of the tidal tensors.

The preferential alignment between $\hat{\mathbf{L}}$ and $\hat{\mathbf{T}}$ can be also quantified in terms of the azimuthal angle ϕ of $\hat{\mathbf{L}}$ in the principal axis frame of $\hat{\mathbf{T}}$. If $\hat{\mathbf{L}}$ is preferentially aligned with the intermediate principal axis of $\hat{\mathbf{T}}$ (i.e., $c \neq 0$), then the probability density distribution $p(\phi)$ should also deviate from the uniform distribution but increases toward $\phi = 90$ in unit of degree: Using equation (4) with $\cos \alpha \equiv \sin \theta \cos \phi$ and $\cos \beta \equiv \sin \theta \sin \phi$, one can derive the azimuthal angle distribution $p(\phi)$ as

$$p(\phi) = \frac{2}{\pi} (1 + c) \sqrt{1 - \frac{c}{2}} \int_0^1 \left[1 + c \left(1 - \frac{3}{2} \sin^2 \theta \sin^2 \phi \right) \right]^{-3/2} d \cos \theta, \quad (6)$$

where ϕ is also assumed to be in the range of $[0, 90]$ in unit of degree for the same reason explained in the above.

The tidal torque theory itself provides little guide in determining the true value of c since it includes the nonlinear effects after the turn-around moment. Thus, the true value of c has to be determined empirically from the observed galaxies. An optimal formula for the determination of c was derived as (Lee & Pen 2001)

$$c = \frac{10}{3} - 10 \sum_{i=1}^3 |\hat{\lambda}_i|^2 |\hat{L}'_i|^2 \quad (7)$$

where (\hat{L}'_i) is the unit galaxy spin measured in the principal axis frame of the tidal shear. For a given sample of N_g galaxies, the statistical errors involved in the measurement of c was also found ¹ to be $\sigma_c = 10/(3\sqrt{5N_g})$ (see Appendix in Lee & Pen 2001).

¹In the original derivation of Lee & Pen (2001) the formula for the statistical error is found for the reduced correlation parameter $a = 5c/3$.

3. OBSERVATIONAL RESULTS

3.1. The Tully Catalog

The optimal data for the measurement of galaxy spins would be a sample of spiral galaxies at low-redshifts ($z < 0.1$). The low-redshift condition is necessary since at high redshifts ($z \geq 0.1$) the weak gravitational lensing shear must cause extrinsic alignments of the galaxy spins (e.g., Crittenden et al. 2001). Here, we adopt the Tully whole sky catalog as an optimal data, which compiles 35,000 local galaxies observed in the northern and southern celestial hemispheres with mean redshift of $\bar{z} \approx 0.4$ (Nilson 1974; Lauberts 1982). For each galaxy, the catalog provides information on the supergalactic positions, equatorial declination (DEC), right ascension (RA), magnitude, velocity, redshift, morphological type, axial ratio (b/a) and position angle (PA). Among the 35,000 galaxies, we restrict our attention only to spiral galaxies with morphological types of 0-9 as listed in Third References Catalog of Bright Galaxies (RC3 de Vaucouleurs et al. 1991). The RC3 morphological types of 0-9 correspond to the Hubble types of S0-Sm. A total of 12122 spiral galaxies with median redshift of ~ 0.02 are selected from the Tully Catalog.

If a spiral galaxy were a thin circular disk, then the cosine of its inclination angle would be nothing but its axial ratio, so that its spin axis could be determined from the given information on its axial ratio (b/a) and position angle (PA) (e.g., Pen et al. 2000; Trujillo et al. 2006). In practice, however, due to the disk's finite thickness and existence of bulge the axial ratio of a spiral galaxy is likely to be under-estimated or over-estimated depending on its type, which would in turn cause non-negligible systematic errors in the measurement of the galaxy's spin axes.

Nevertheless, it is possible to minimize the systematic errors caused by the limited validity of the thin-disk approximation if the morphological type of the spiral galaxy is known: Haynes & Giovanelli (1984) provided corrections to the inclination angle, i , of a spiral galaxy by adding an intrinsic flatness parameter, p , as:

$$\cos^2 i = \frac{(b/a)^2 - p^2}{1 - p^2}. \quad (8)$$

According to Haynes & Giovanelli (1984), the value of the intrinsic flatness parameter, p , varies with galaxy morphological type as

$$\begin{aligned} p &= 0.23, & \text{S0} - \text{Sa} \\ &= 0.20, & \text{Sab} \\ &= 0.175, & \text{Sb} \\ &= 0.14, & \text{Sbc} \end{aligned}$$

$$\begin{aligned}
&= 0.103, \quad \text{Sc} \\
&= 0.10, \quad \text{Scd} - \text{Sdm}
\end{aligned}$$

The value of i is set to $\pi/2$ if $b/a < p$.

Adopting the above correction given by Haynes & Giovanelli (1984), the spin axis of a spiral galaxy in the local spherical polar coordinate system can be written as

$$\hat{L}_r = \cos i, \quad \hat{L}_\vartheta = (1 - \cos^2 i)^{1/2} \sin PA, \quad \hat{L}_\varphi = (1 - \cos^2 i)^{1/2} \cos PA \quad (9)$$

where $(\hat{L}_r, \hat{L}_\vartheta, \hat{L}_\varphi)$ represents the three components of the unit spin vector in the local spherical polar coordinate system. It is worth mentioning here that the spin vector determined from equation (9) suffers from the sign ambiguity in \hat{L}_r , as mentioned in (Pen et al. 2000; Trujillo et. al. 2006). Since it is not possible to determine the sign of \hat{L}_r from the given information of the Tully Catalog, we apply positive sign to all Tully galaxies here. We expect that this sign ambiguity will play a role of decreasing the strength of the spin-shear alignment signal.

Now, the equatorial Cartesian coordinates of the unit spin vector, $(\hat{L}_1, \hat{L}_2, \hat{L}_3)$, can be determined by using the given information on *DEC* and *RA*:

$$\begin{aligned}
\hat{L}_1 &= \hat{L}_r \sin \vartheta \cos \varphi + \hat{L}_\vartheta \cos \vartheta \cos \varphi - \hat{L}_\varphi \sin \varphi, \\
\hat{L}_2 &= \hat{L}_r \sin \vartheta \sin \varphi + \hat{L}_\vartheta \cos \vartheta \sin \varphi + \hat{L}_\varphi \cos \varphi, \\
\hat{L}_3 &= \hat{L}_r \cos \vartheta - \hat{L}_\vartheta \sin \vartheta
\end{aligned} \quad (10)$$

where $\vartheta = \pi/2 - \text{DEC}$ and $\varphi = \text{RA}$.

Rotating the spin axis from the equatorial to the supergalactic coordinate system, we finally measure the spin axis of each Tully spiral galaxy in the supergalactic coordinate system. We measure the spin-shear alignments in the supergalactic coordinate system since the 2MRS density field is defined in the supergalactic coordinate system.

3.2. The 2MRS Tidal Field

An optimal data for the measurements of the tidal shear tensors would be the linear tidal field calculated in real space. We use the data from the Two Mass Redshift Survey (2MRS) which is the densest redshift survey to date, mapping all of the sky in the infrared bands out to a median redshift of $z = 0.02$ (Huchra et al. 2005). By expanding the 2MRS data in Fourier-Bessel functions, the real-space density field, $\delta(\mathbf{x})$, was constructed on 64^4 pixels in

a regular cube of linear size $400h^{-1}\text{Mpc}$ in supergalactic coordinate system (Erdogdu et al. 2006).

To construct the tidal shears from the 2MRS density field, we first calculate the Fourier-transform of the density field, $\delta(\mathbf{k})$, using the Fast-Fourier-Transformation (FFT) method (Press et al. 1992). Since the tidal tensor is defined as the second derivative of the gravitational potential, the Fourier transform of the density field is related to the Fourier transform of the tidal shear field $T_{ij}(\mathbf{k})$ as $T_{ij}(\mathbf{k}) = k_i k_j \delta(\mathbf{k}) / k^2$. Then, we perform the inverse Fourier-transformation of $T_{ij}(\mathbf{k})$ to construct the tidal shear field in real space, $T_{ij}(\mathbf{x})$, on the same cube with 64^3 pixels.

With the reconstructed 2MRS tidal shear field, we calculate the tidal tensor at the positions of the selected Tully galaxies by means of the Cloud-in-Cell (CIC) interpolation method (Hockney & Eastwood 1988). For a given supergalactic position \mathbf{x}_p of each selected Tully galaxy, we first find the eight nearest pixels. And then we interpolate the tidal tensors at the eight pixels to evaluate the value of $T_{ij}(\mathbf{x}_p)$. We subtract the trace from $T_{ij}(\mathbf{x}_p)$ and normalize it to have unit magnitude. Diagonalizing the unit traceless tidal tensor $\hat{T}_{ij}(\mathbf{x}_p)$ at the position of a selected Tully galaxy, we find the three eigenvalues $\{\hat{\lambda}_1, \hat{\lambda}_2, \hat{\lambda}_3\}$ and the corresponding three eigenvectors as well $\{\mathbf{e}_1, \mathbf{e}_2, \mathbf{e}_3\}$.

3.3. The Observed Spin-Shear Alignments

3.3.1. The mean value of the correlation parameter

Now that the spin vectors and the tidal tensors are all found at the supergalactic positions of the Tully spiral galaxies, we are ready to measure the alignments between the spin axes and the principal axes of the tidal tensors.

Let α , β , and θ represent the angles between the spin axis of a given Tully galaxy with the major, intermediate, and minor principal axis of the local tidal tensor, respectively: $\cos \alpha \equiv |\hat{\mathbf{L}} \cdot \mathbf{e}_1|$; $\cos \beta \equiv |\hat{\mathbf{L}} \cdot \mathbf{e}_2|$; $\cos \theta \equiv |\hat{\mathbf{L}} \cdot \mathbf{e}_3|$. Here, the angle ϕ is the azimuthal angle of the spin axis in the $\hat{\lambda}_1$ - $\hat{\lambda}_2$ plane. Note that the three angles α , β and θ are forced to be in the range of $[0, 90]$ in unit of degree since what is relevant to us is not the sign of a spin vector but its spatial orientation relative to the principal axes of the tidal tensor.

For each Tully galaxy, we calculate $\cos \alpha$, $\cos \beta$, and $\cos \theta$ and determine their probability density distributions. Figure 1 plots the results as solid dots with Poisson errors in the left, middle and right panels, respectively. As can be seen, the galaxy spin axes are indeed preferentially aligned with the *intermediate* principal axes of the local tidal tensors, which

is consistent with theoretical prediction presented in §2. With the help of a Kolmogorov-Smirnov test, we find that the null hypothesis of no spin-shear alignment is rejected at 99.99% confidence level.

Through the similarity transformation, we express the spin vector of each selected galaxy in the principal axis frame of the tidal shear tensor, $\hat{\mathbf{L}}'$. Then, we evaluate the correlation parameter c by equation (7). The mean value of c is found to be $\bar{c} = 0.084 \pm 0.014$. Although the value of c itself is quite low, it is $6\sigma_c$ deviation from zero, which marks a detection of the intrinsic spin-shear alignments at present epoch.

Figure 2 compares the observational results (solid dots) with the analytic model (solid line). To calculate the analytic model we put the mean value of $\bar{c} = 0.084 \pm 0.014$ determined from the observational data into equation (5). The dotted line corresponds to the case of no correlation. As can be seen, the analytic model agrees with the observational results quite well.

We also measure the probability distribution of the azimuthal angle ϕ of the spin axes in the tidal shear principal axis frame. Figure 3 plots the results as solid dots and compares it with the analytic model as solid line (eq.6). From the observational results, it is clear that $p(\phi)$ is not uniform but increases as the azimuthal angle increases toward $\phi = 90$ in unit of degree. The analytic model is also in good agreement with the observational result. Although $p(\phi)$ is less steep than $p(\cos \beta)$, this non-uniform distribution of $p(\phi)$ provides an additional evidence for the preferential alignments between the galaxy spin axes and the intermediate principal axes of the tidal tensors. It reveals that the projected orientations of the galaxy spin axes onto the plane perpendicular to the minor principal axes of the local tidal field are anisotropic toward the directions of the intermediate principal axes of the tidal field.

3.3.2. Dependence on the morphology

It has already been noted by previous works that the orientation of the galaxy spin axes may depend crucially on the galactic morphology and type: Flin & Godlowski (1986, 1990) showed that the orientations of the galaxy spin axes in the Local Supercluster (LSC) tend to lie on the plane of the Local Supercluster, the distribution of which depends on whether the galaxies are seen face-on or edge-on. Recently, Aryal & Saurer (2005b) found that the spiral galaxies in the LSC are observed to have anisotropic spin orientations relative to the plane of LSC, while the barred spiral and irregular galaxies exhibit no signal of anisotropic spin orientations. Since the LSC is likely to have formed through the gravitational

collapse along the major principal axes of the local tidal field, these previous results on the anisotropic galaxy orientations relative to the LSC provide indirect observational evidences for the morphological dependence of the intrinsic galaxy correlations with the local tidal field.

Here, we would like to investigate more directly how the intrinsic alignment of the galaxy spin axes with the tidal field depends on the galaxy morphology. To investigate how the value of c changes with the morphological type, we classify the Tully spiral galaxies into four samples with morphological types given as 0-1 (S0-Sa); 2-3 (Sab-Sb); 4-5 (Sbc-Sc); 6-9 (Scd-Sm). Then, for each sample we measure $p(\cos\beta)$, $p(\phi)$ and c separately.

The observational results of $p(\cos\beta)$ and $p(\phi)$ are plotted as solid dots in Figs. 4 and 5, respectively. In each Figure, the analytic models are also plotted as solid line. Table 1 lists the number of galaxies (N_g) and the mean value of c for the four samples. For the calculation of the analytic model, we use the mean value of \bar{c} listed in the third column.

As can be seen, the value of c does not depend strongly on the morphological type of the spiral galaxy. But, it tends to decrease slightly as the type increases. The value of the correlation parameter c is as low as 0.05 for the galaxy sample of types 6-9. This result suggests that the intrinsic spin-shear correlation is stronger for the massive galaxies. A possible explanation for this phenomenon is that the massive galaxies are usually located in high-density regions and thus they experienced stronger tidal effect from the surrounding matter. As a matter of fact, very recently, Lee & Pen (2007) analyzed the numerical data from high-resolution N-body simulation to find that the value of c increases as the mass of the dark halo increases. Thus, our observational result is consistent with numerical prediction given by Lee & Pen (2007).

Fig. 5 shows that the non-uniform distribution of $p(\phi)$ can be seen only for the galaxy samples of types 2 – 5. However, for the case of $p(\phi)$ which is less steep than $p(\cos\beta)$, the large Poisson errors make it difficult to detect clearly the signal of the morphological dependence of $p(\phi)$, even though it exists, due to the small number of galaxies in the samples.

3.3.3. Dependence on the environment

To examine the environmental dependence of the correlation parameter c , we classify the Tully spiral galaxies into two samples belonging to the overdense region ($\delta < \bar{\delta}$) and to the underdense-region ($\delta > \bar{\delta}$) where $\bar{\delta}$ is the mean density of the 2MRS density field. Then we measure $p(\cos\beta)$, $p(\phi)$ and c for each sample separately.

The observational results of $p(\cos \beta)$ and $p(\phi)$ are plotted as solid dots in Figs. 6 and 7, respectively. In each Figure, the analytic models are also plotted as solid line. Table 2 lists the number of galaxies (N_g) and the mean value of c for the four samples.

As can be seen, the value of c is much larger in the overdense regions than in the underdense regions, indicating that the intrinsic spin-shear correlation is stronger for those galaxies which are located in the overdense regions. A possible explanation is that in the overdense regions the galaxies experience stronger tidal torques from the surrounding matter and thus have kept its memory of the tidal interaction better.

It is worth mentioning that in the bottom panel of Fig. 7 the observational result of $p(\phi)$ has a non-negligible hump around $\phi = 30$ degree, which looks inconsistent with the analytic model. However, recall the fact that the distribution, $p(\phi)$, corresponds to the alignments of the projected spin axes (as mentioned in §3.3.1 -2) and thus it is less steep than $p(\cos \beta)$. In other words, it suffers more severely from the small number statistics. Since the number of the galaxies, N_g , which belong to the low-density environment is quite small and the value of c has a large error for this case, this hump can be interpreted as a statistical fluctuation within errors.

4. SUMMARY AND CONCLUSION

The achievements of our work are summarized as

- We have measured the intrinsic alignments between the spin axes of the nearby spiral galaxies from the Tully Galaxy Catalog and the principal axes of the local tidal tensors reconstructed from the 2MRS density field. We have detected a clear signal of the intrinsic alignments between the spin axes of the spiral galaxies and the intermediate principal axes of the local tidal tensors. The signal is statistically significant at 6σ level.
- It has been found that the signal of the intrinsic spin-shear correlation depends weakly on the morphological type of the spiral galaxy. It is stronger for the early type spiral galaxies. This result is consistent with numerical experiment.
- It has been found that the signal depends on the local density. It is stronger in the overdense regions, which can be understood as the galaxies in the overdense regions experience stronger tidal effect from the surrounding matter.
- Our results provide a compelling evidence for the tidal torque scenario that the galaxy spins indeed originated from the initial tidal interaction with the surrounding matter.

- Since a significant signal of the tidal alignments of the blue galaxies is detected, it will be useful for the weak lensing analyses since it has been regarded as possible contaminants of the weak lensing signals (e.g., Hirata et al. 2007).

A final conclusion is that since the present galaxy spin field still keeps the memory of the initial tidal interaction, it is another fossil record of the density field at early epochs when the proto-galaxies were in expansion stages. Thus, the galaxy spin field can be in principle used as a new complimentary probe of the dark matter distribution in the universe, as proposed by Lee & Pen (2000, 2001)

We are very grateful to an anonymous referee who helped us improve the original manuscript significantly. J.L. thanks B. Tully for the galaxy catalog and stimulating discussions. P.E. thanks the 2MRS team for their contributions to the reconstruction of the 2MRS density field. J.L. acknowledges the financial support from the Korea Science and Engineering Foundation (KOSEF) grant funded by the Korean Government (MOST, NO. R01-2007-000-10246-0).

REFERENCES

- Aryal, B., & Saurer, W. 2005a, MNRAS, 360, 125
- Aryal, B., & Saurer, W. 2005b, A&A, 432, 431
- Aragon-Calvo, M. A., van de Weygaert, R., Jones, B. J. T., & van der Hulst, J. M. 2007, ApJ, 655, 5
- Brunino, R., Trujillo, I., Pearce, F. R. & Thomas, P. A. 2007, MNRAS, 375, 184
- Crittenden, R. G., Natarajan, P., Pen, U. L & Theuns, T. 2001, ApJ, 559, 552
- de Vaucouleurs, G., de Vaucouleurs, A., Corwin, H. G., Jr., Buta, R. J., Patuerl, G. & Fouque, P. 1991, Third Reference Catalogue of Bright Galaxies (New York:Springer)
- Doroshkevich, A. G. 1970, Astrofizika, 6, 581
- Dubinski, J. 1992, ApJ, 401, 441
- Erdogdu, P. et al. 2006, MNRAS, 373, 45
- Flin, P. & Godlowski, W. 1986, MNRAS, 222, 525

- Flin, P. & Godlowski, W. 1990, *Soviet Astr. Lett.*, 16, 209
- Guth, A. H. & Pi, S. Y. 1982, *Phys. Rev. Lett.*, 49, 1110
- Hahn, O., Porciani, C., Carollo, C. M., & Dekel, A. 2007, *MNRAS*, 375, 489
- Haynes, M. P. & Giovanelli, R. 1984, *AJ*, 89, 758
- Hirata, C. et al. 2007, preprint [astro-ph/0701671]
- Hockney, R. W. & Eastwood, J. W. 1988, *Computer Simulation Using Particles* (New York: Taylor & Francis)
- Huchra, J. et al. 2005, in *Nearby large scale structures and the zone of avoidance* (ed. Fairall, F. & Woudt, P. A.) 135-142 (ASP Conf. Ser. 329, Astronomical Society of the Pacific, Cape Town)
- Jing, Y. 2002, *ApJ*, 335, L89
- Lauberts, A. 1982, *ESO/Uppsala Survey of the ESO(B) Atlas*. (Garching:ESO)
- Lee, J., Kang, X., & Jing, Y. 2005, *ApJ*, 629, L5
- Lee, J. & Pen, U. L. 2000, *ApJ*, 532, L5
- Lee, J. & Pen, U. L. 2001, *ApJ*, 555, 106
- Lee, J. & Pen, U. L. 2002, *ApJ*, 567, 111
- Lee, J. & Pen, U. L. 2007, preprint [arXiv:0707.1690]
- Mo, H. J., Mao, S. & White, S. D. M. 1998, *MNRAS*, 295, 319
- Navarro, J.F., Abadi, M.G., & Steinmetz, M. 2004, *ApJ*, 613, L41
- Nilson, P. 1974, *Uppsala Astron. Obs. Ann.*, 6
- Patiri, S. G., Cuesta, A. J., Prada, F., Betancort-Rijo, J., & Klypin, A. 2006, *ApJ*, 652, 75
- Peebles, P. J. E. 1969, *ApJ*, 155, 393
- Pen, U. L., Lee, J., & Seljak, U. 2000, 543, L107
- Porciani, C., Dekel, A., & Hoffman, Y. 2002, *MNRAS*, 332, 339

- Press, W. H., Teukolsky, S. A., Vetterling, W. T. & Flannery, B. P. 1992, Numerical Recipes in FORTRAN (Cambridge : Cambridge Univ. Press)
- Trujillo, I., Carretero, C., & Patiri, S. 2006, ApJ, 610, L111
- Vitvitska, M., Klypin, A. A., Kravtsov, A. V., Wechsler, R. H., Primack, J. R. & Bullock, J. S. 2002, ApJ, 581, 789
- White, S. D. M. 1984, ApJ, 286, 38
- Wittman, D. M., Tyson, J. A., Kirkman, D., Dellantonio, I. & Bernstein, G. 2000, Nature, 405, 143

Table 1. The galaxy’s morphological type, the number of the Tully galaxies (N_g), and the mean value of the correlation parameter (c).

Types	N_g	\bar{c}
All	12122	0.084 ± 0.014
S0,Sa	1761	0.105 ± 0.036
Sab,Sb	3175	0.097 ± 0.026
Sbc,Sc	4507	0.082 ± 0.022
Scd,Sd,Sdm,Sm	2679	0.058 ± 0.029

Table 2. The local density, the the number of the Tully galaxies (N_g), and the mean value of the correlation parameter (c).

Environment	N_g	\bar{c}
overdense ($\delta > \bar{\delta}$)	8249	0.108 ± 0.016
underdense ($\delta < \bar{\delta}$)	3873	0.033 ± 0.024

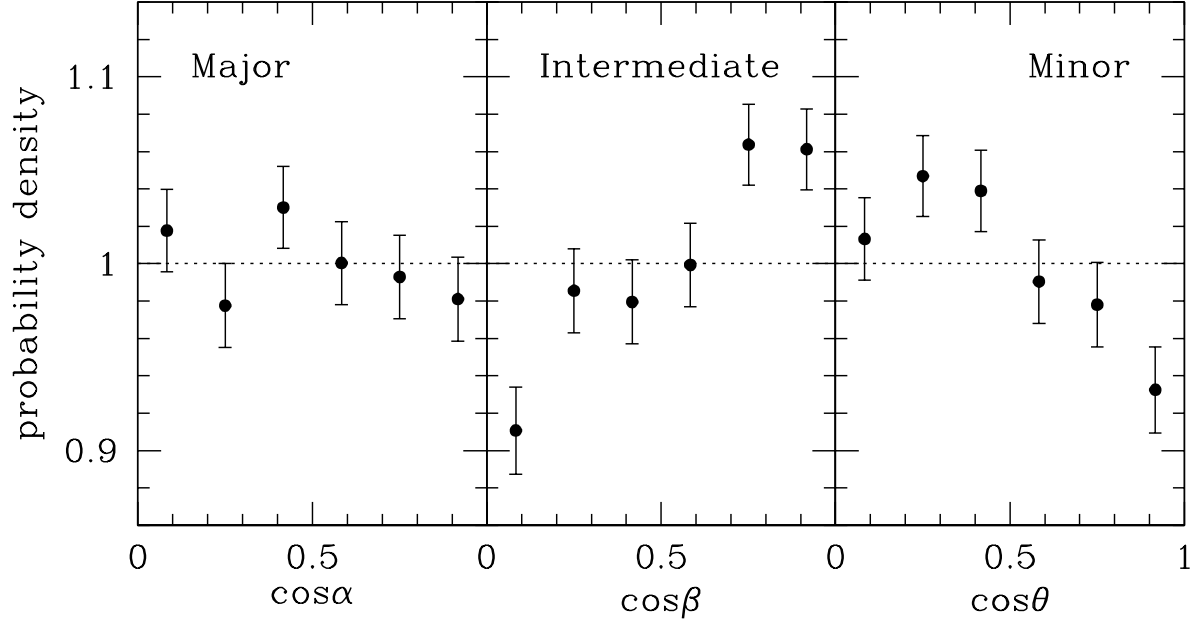


Fig. 1.— Probability density distribution of the cosines of the angles between the spin axes of the Tully spiral galaxies and the major, intermediate, and minor principal axes of the local tidal tensors, in the left, middle, and right panel, respectively.

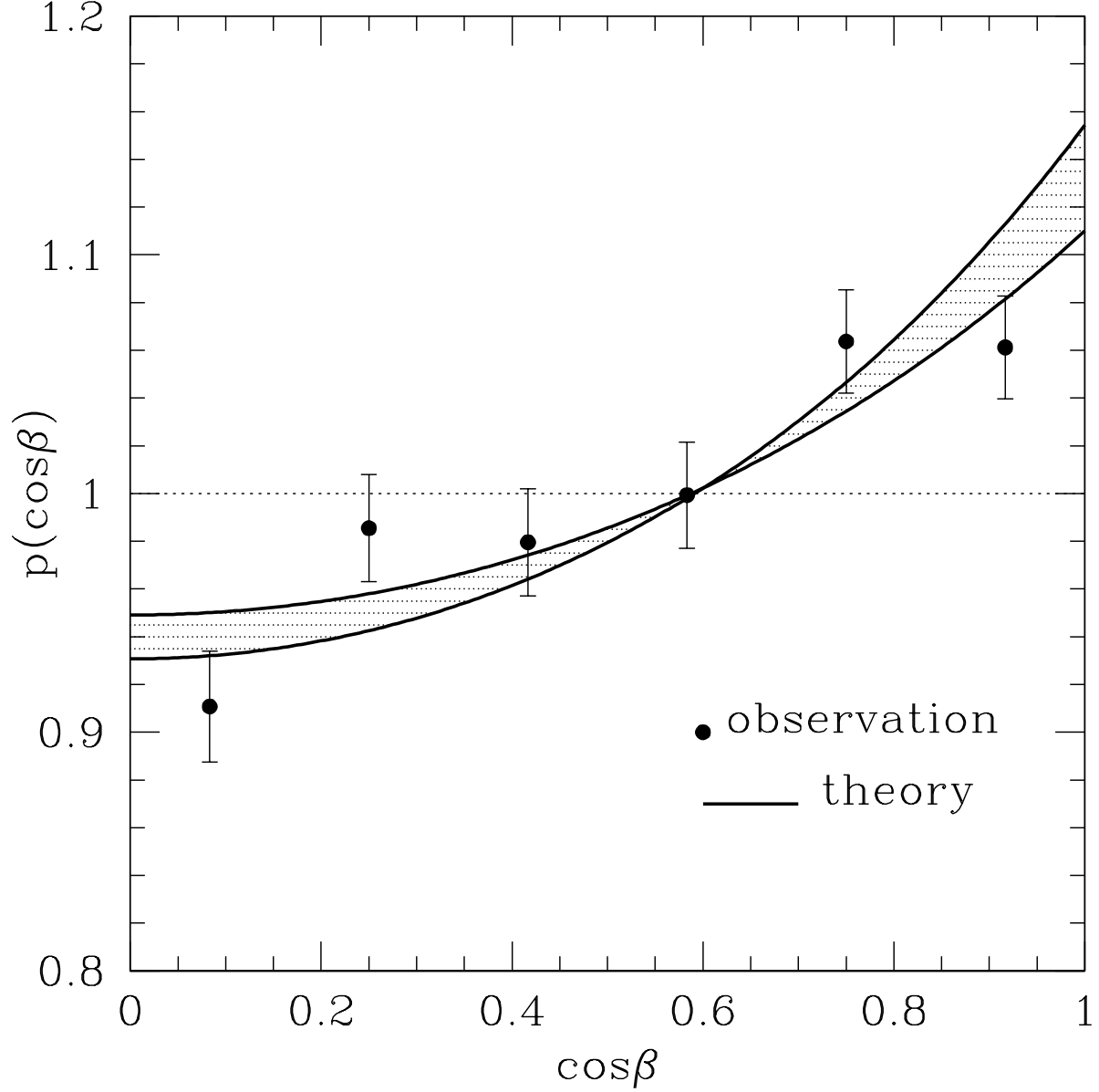


Fig. 2.— Probability density distribution of the cosines of the angles between the spiral galaxy’s spin axes and the intermediate principal axes of the local tidal tensors. The solid dots with Poisson errors represent the observational results, the solid lines correspond to the analytic predictions, and the dotted line represents the case of no correlation. The shaded area represents 1σ of the correlation parameter. A total of 12347 spiral galaxies with all morphological types are used.

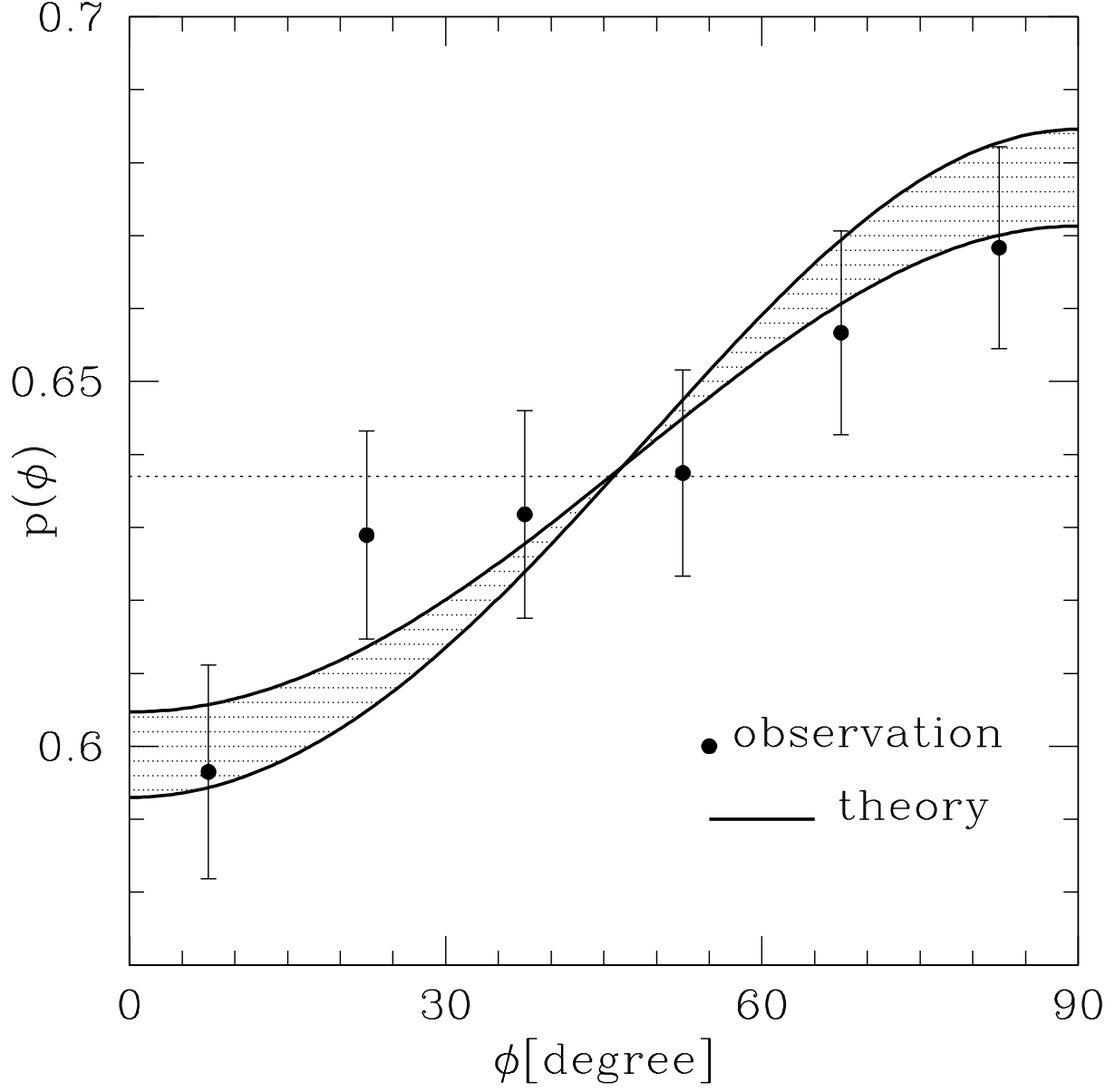


Fig. 3.— Probability density distribution of the azimuthal angles of the galaxy’s spin axes in the principal axis frame of the local tidal shear tensors.

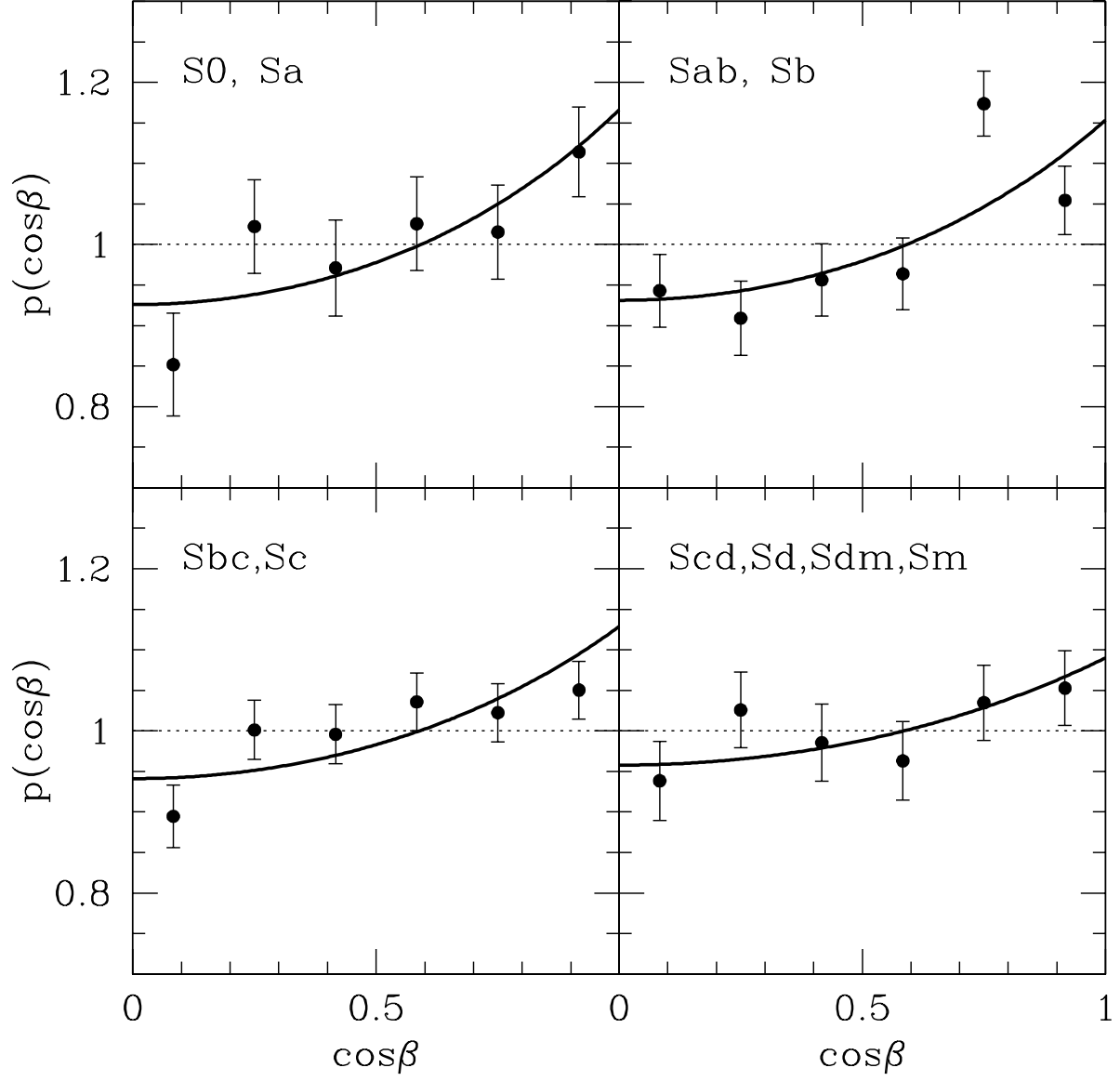


Fig. 4.— Same as Fig. 2 but for the different cases of the galaxy's morphological types: types of S0-Sa (top-left); types of Sab-Sb (top-right); types of Sbc-Sc (bottom left); types of Scd-Sm (bottom right).

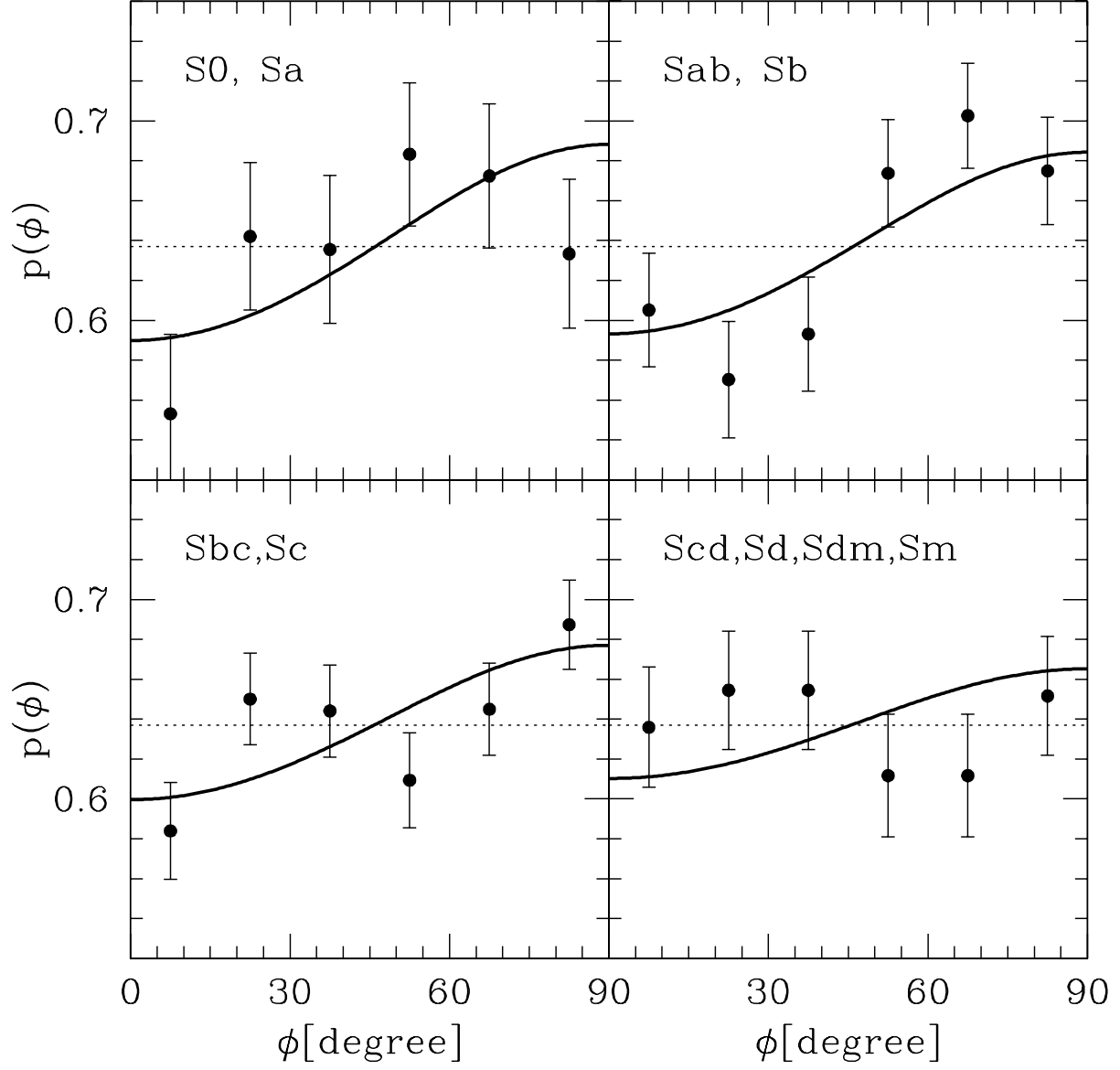


Fig. 5.— Same as Fig. 3 but for the different cases of the galaxy’s morphological types: types of S0-Sa (top-left); types of Sab-Sb (top-right); types of Sbc-Sc (bottom left); types of Scd-Sm (bottom right).

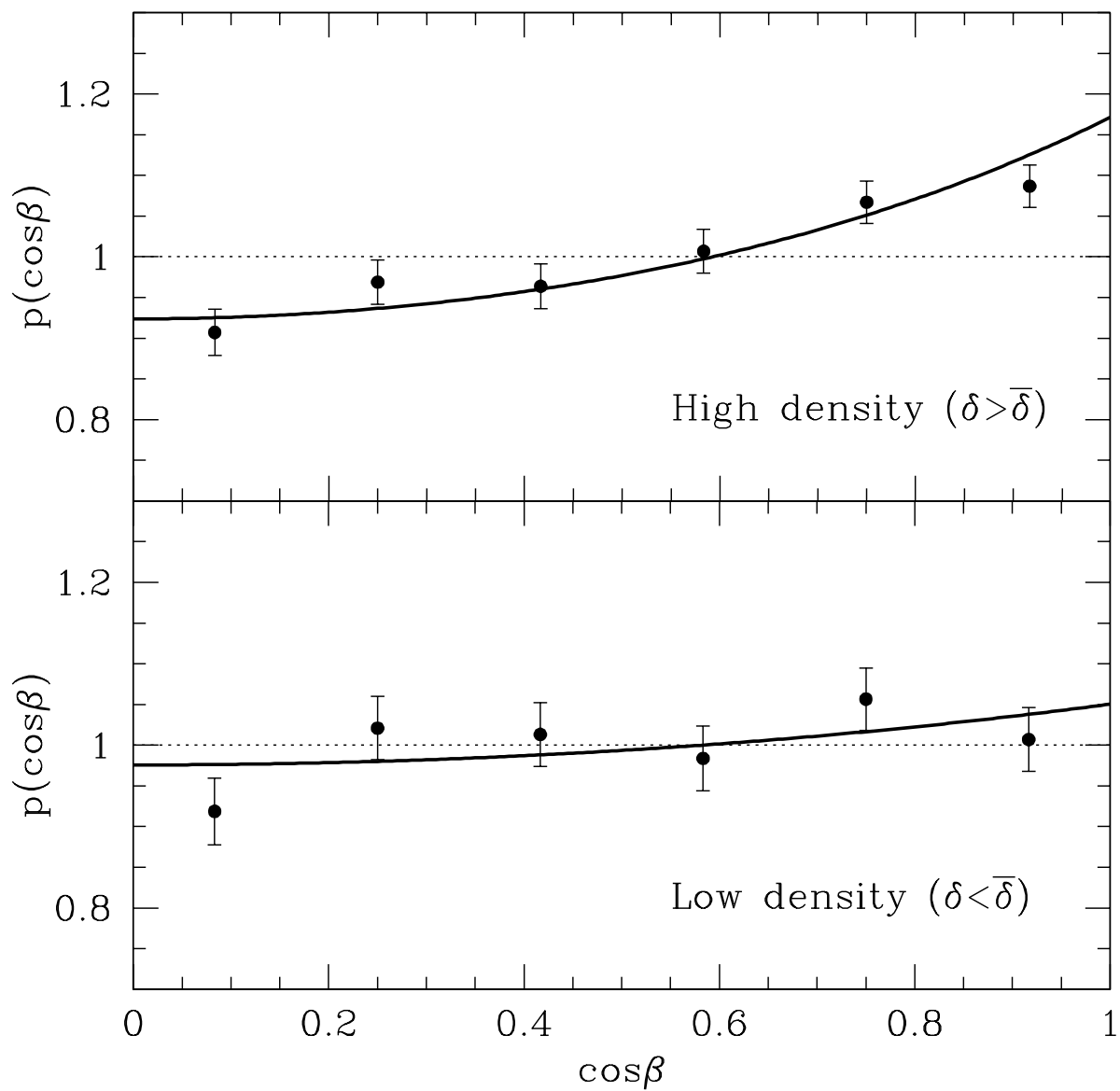


Fig. 6.— Same as Fig.2 but for the two different cases of the local density contrast: overdense (top) and underdense (bottom).

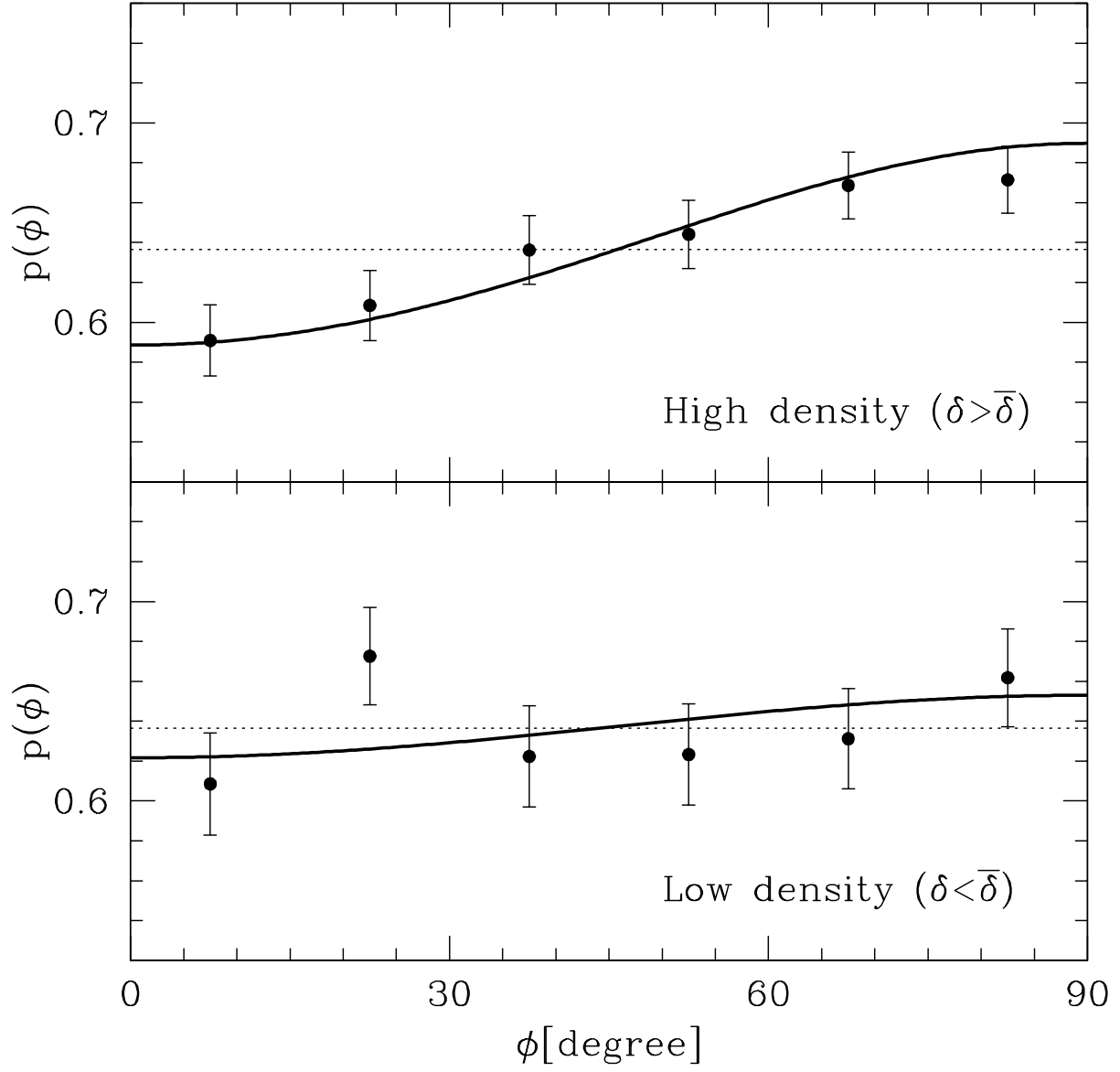


Fig. 7.— Same as Fig.3 but for the two different cases of the local density contrast: overdense (top) and underdense (bottom).